Coupling Efficiency Between Optical Fiber and Ti:$LiNbO_3$ Channel Waveguide

Marcos Antonio Ruggieri Franco[1,2], Laurentino C. de Vasconcellos[1], and José Márcio Machado[3]

[1] Instituto de Estudos Avançados – IEAv/CTA, 12228-840 São José dos Campos–SP, Brazil
[2] also with Instituto Tecnológico de Aeronáutica – ITA, São José dos Campos –SP, Brazil
[3] Depto. de Ciências da Computação e Estatística IBILCE – UNESP, Brazil.

Abstract — The coupling efficiency between a single-mode circular core optical fiber and a single-mode (E^x) Ti:$LiNbO_3$ channel waveguide is calculated as a function of the diffusion process parameters. The waveguide modal analysis was carried out by the finite element method and the fiber to waveguide coupling efficiency was evaluated by the overlap integral factor.

Index Terms — Finite element method, integrated optics, optical fiber coupling, waveguides.

I. Introduction

The development of low-cost photonic integrated devices for future wide-scale commercialization requires an efficient coupling between the single-mode optical fibers and the optical waveguides as well as a large mechanical alignment tolerance.

Among the several causes of losses in the connection of a fiber and a waveguide, the main causes are the mode field mismatch, the transversal offset, the longitudinal separation, the angular offset, and the refractive index mismatch [1]-[3]. From these, the mode-field mismatch and the relative alignment are the principal sources of fiber-to-waveguide coupling losses. The alignment is typically at least ten times more demanding than the tolerances for integrated circuit packaging. Therefore, the alignment and attachment of fibers are the most difficult challenges facing the optical device packaging.

The analyses of fiber-to-waveguide coupling losses were presented by the several authors [1]-[12]. In the majority of these papers, the coupling efficiency was calculated for z-cut $LiNbO_3$ substrates using approximating functions to represent the fiber and waveguide mode-field profiles.

In this work, the coupling efficiency between a single-mode circular core optical fiber and a single-mode (E_{11}^x) Ti:$LiNbO_3$ waveguide was calculated by the overlap integral of the spatial field distribution. For the circular core fiber, the field profile was approximated by the Gaussian function, and for the waveguide formed by diffused Ti-ions on x-cut $LiNbO_3$ substrate the mode field profile was determined by the finite element method [13]. The coupling efficiency calculations were performed as a function of the initial Ti-strip geometry and the diffusion process parameters. The alignment tolerances in the transversal plane were also determined.

The fiber-to-waveguide attachment scheme and the system reference for the relative alignment are presented in the Fig. 1.

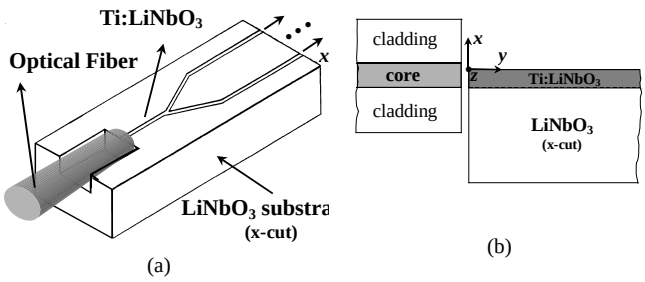

Fig. 1. "End-fire" fiber-to-waveguide coupling. (a) Attached single-mode circular core fiber to Ti:$LiNbO_3$ waveguide device, (b) Longitudinal view of the relative alignment between fiber and waveguide.

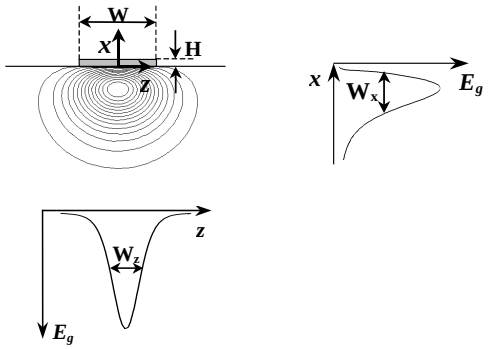

Fig. 2. Initial geometrical parameters of the Ti-strip and guided optical field profile in the diffused Ti:$LiNbO_3$ waveguide. W_x and W_z are the mode diameter at half maximum of the optical electric field (E_g) intensity.

II. Ti:$LiNbO_3$ Channel Waveguide

Optical waveguides formed by diffusion of Ti-ions in $LiNbO_3$ substrate are widely used in the optical integrated circuits. The controllable diffusion parameters determine the mode shape and the confinement. To define the optical channel waveguide, the following manufacturing parameters were taken into account: the initial width (W) and thickness (*H*) of the Ti-strip, the ion diffusion temperature (*T*) and the ion diffusion time (*t*). The calculations were performed for a guide built in an x-cut y-propagation $LiNbO_3$ substrate for a wavelength of 1.523 μm.

The schematic view of the initial Ti-strip-geometrical parameters, the fundamental mode (E_{11}^x) electric field contour lines and the field-profile in the transversal directions are shown in Fig. 2. Because of the anisotropic

Ti-diffusion characteristic, the mode field presents a nonsymmetrical shape. The W_x and W_z are the mode diameters defined as the full width at half maximum of the field intensity in the transversal directions *z* and *x*.

For Ti:$LiNbO_3$ channel waveguides, the refractive index in the diffused region follows [14]:

$$n_{e,o}^2(x,z,\lambda) = n_{b_{e,o}}^2 + \left[\left(n_{b_{e,o}} + \Delta n_{s_{e,o}}\right)^2 - n_{b_{e,o}}^2\right] \exp\left(-\frac{x^2}{d_x^2}\right) f\left(\frac{2z}{W}\right) \quad (1)$$

where:

$$f\left(\frac{2z}{W}\right) = \frac{1}{2}\left\{erf\left[\frac{W}{2d_z}\left(1+\frac{2z}{W}\right)\right] + erf\left[\frac{W}{2d_z}\left(1-\frac{2z}{W}\right)\right]\right\},$$

e, *o* denote the extraordinary and ordinary rays respectively, *x* and *z* are the coordinates of a point in the substrate, d_z and d_x are the diffusion width and depth respectively, n_b is the substrate refractive index, Δn_s is the variation of the surface index with the wavelength and $f(2z/W)$ represents the solution of the anisotropic diffusion problem.

In addition, $\Delta n_{S_{e,o}}$ is given in terms of *H* and some fitting parameters [15]:

$$\Delta n_{s_{e,o}}(\lambda) = \left[B_0(\lambda) + B_1(\lambda)\frac{H}{d_{x_{e,o}}}\right]\left(\frac{H}{d_{x_{e,o}}}\right)^{\alpha_{e,o}}, \quad (2)$$

α_e=0.83, α_o=0.53, $0.6 \le \lambda\ (\mu m) \le 1.6$,

$B_{0e}(\lambda)$= 0.385 − 0.430λ + 0.171λ^2,

$B_{1e}(\lambda)$=9.130+3.850λ−2.490λ^2,

$B_{0o}(\lambda)$=0.0653−0.0315λ+0.0071λ^2,

$B_{1o}(\lambda) = 0.4780 + 0.4640\ \lambda - 0.3480\ \lambda^2$.

The diffusion coefficients D_z and D_x, the diffusion width d_z and depth d_x, and the depths of refractive index change profiles d_{xe} and d_{xo} can be calculated by [15]:

$$D_i = D_{i0}\exp\left(-E_{i0}/kT\right), \quad i=x,z \quad (3)$$

$$d_i = 2\sqrt{D_i t}\,, \quad i=x,\ z \quad (4)$$

$$d_{xe,o} = \frac{d_x}{\sqrt{\alpha_{e,o}}}, \quad (5)$$

where D_{i0} is the diffusion constant, E_{i0} is the activation energy and *k* is the Boltzmann constant. These constants for Ti:$LiNbO_3$ waveguides are presented in Table I [15].

The refractive indexes dispersion of the $LiNbO_3$ are taken into account by using (6) and (7) with the wavelength (λ) in μm [16], and they are:

$$n_{b_o}^2 = 4.9048 - \frac{0.11768}{0.04750 - \lambda^2} - 0.027169\ \lambda^2, \quad (6)$$

$$n_{b_e}^2 = 4.5820 - \frac{0.099169}{0.044432 - \lambda^2} - 0.021950\ \lambda^2. \quad (7)$$

III. FINITE ELEMENT MODEL

The modal analysis of the Ti:$LiNbO_3$ waveguide was carried out by a scalar finite element implementation both for nonhomogeneous and anisotropic media [13]. Accurated optical field profile and propagation constants can be obtained by the application of the finite element method.

TABLE I

COEFFICIENTS OF THE ARRHENIUS LAW FOR Ti:$LiNbO_3$ GUIDES

D_{z0} (μm² / h)	5.0 e+9
D_{x0}(μm² / h)	1.35 e+8
E_{z0} (eV)	2.60
E_{x0} (eV)	2.22

The Helmholtz equation in the scalar approximation, for a lossless, inhomogeneous and anisotropic dielectric optical waveguide with diagonal permittivity tensor, and a harmonically *y*-propagating wave, can be expressed for the E^x modes as:

$$n_y^2 \frac{\partial}{\partial z}\left(\frac{1}{n_y^2}\right)\frac{\partial\left(n_z^2 E_z\right)}{\partial z} + \frac{\partial^2\left(n_z^2 E_z\right)}{\partial z^2} + n_y^2\frac{\partial^2 E_z}{\partial x^2} + k_0^2 n_z^2 n_y^2 E_z = n_y^2 \beta^2 E_z, \quad (8)$$

and for the E^y modes as follows:

$$\frac{\partial^2 H_z}{\partial z^2} + n_x^2\frac{\partial}{\partial x}\left(\frac{1}{n_y^2}\frac{\partial H_z}{\partial x}\right) + n_x^2 k_0^2 H_z = \beta^2 H_z, \quad (9)$$

where k_0 is the free space wavenumber and β is the propagation constant. The variables $n_x(z,x)$, $n_z(z,x)$ are the refractive indexes in the transversal directions and $n_y(z,x)$ is the refractive index in the longitudinal direction.

The application of the Weighted Residual Method with the Galerkin Approximation in (8) and (9) yields the matrix equation:

$$[F]\{\phi\}^T = n_{eff}^2\,[M]\{\phi\}^T, \quad (10)$$

where $n_{eff} = \beta / k_0$ is the effective index. The matrices for each finite element are given by:

$$[M] = \int_\Omega A\ k_0^2\ \{N\}^T\{N\}\,dz\,dx, \quad (11)$$

$$[F] = [F_1] - [F_2]. \quad (12)$$

For the E^x modes the matrices are:

$$[F_1]=\int_\Omega \left(k_0^2\, n_z^2\, n_y^2 \{N\}^T\{N\} - n_z^2 \{N\}_z^T\{N\}_z\right) dz\, dx - \int_\Omega n_y^2 \{N\}_x^T\{N\}_x\, dz\, dx\,, \quad (13)$$

$$[F_2]=\int_\Omega \left(\delta_z \frac{\partial n_z^2}{\partial z}\{N\}_z^T\{N\} + \delta_y \frac{\partial n_y^2}{\partial x}\{N\}^T\{N\}_x\right) dz\, dx + \int_\Omega \delta_y n_z^2 n_y^2 \frac{\partial g_y^2}{\partial z}\{N\}^T\{N\}_x\, dz\, dx\,. \quad (14)$$

For E^y modes follows:

$$[F_1]=\int_\Omega \left[k_0^2\, n_x^2\, \{N\}^T\{N\} - \{N\}_z^T\{N\}_z\right] dz\, dx - \int_\Omega n_x^2\, g_y^2 \{N\}_x^T\{N\}_x\, dz\, dx\,, \quad (15)$$

$$[F_2] = \int_\Omega \left[\delta_z\, g_y^2 \frac{\partial n_x^2}{\partial x} + \delta_y\, n_x^2 \left(\frac{\partial g_y^2}{\partial x} + g_y^4 \frac{\partial n_y^2}{\partial x}\right) \{N\}^T\{N\}_x\right] dz\, dx\,, \quad (16)$$

where $A = n_z^2$, for E^x modes, or $A = 1$, for E^y modes, $g_y = 1/n_y$, $\{N\}_x = \partial\{N\}/\partial x$ and $\{N\}_y = \partial\{N\}/\partial y$ and x and z are the transversal axis and y is the propagation direction. The parameters δ_z and δ_x assume either the value 1 for diffused index in the z and x directions respectively, or zero for constant index. The matrix $[F_2]$ is sparse and nonsymmetrical because of the presence of terms with refractive index partial derivative.

In this work, the variation of the refractive indexes and their spatial derivatives inside each finite element are expanded in terms of the base functions $\{N\}$:

$$n_i^2 = \{N\}\left\{n_i^2\right\}^T, \quad i, j = x, y, z$$

$$\frac{\partial n_i^2}{\partial j} = \{N\}\left\{n_i^2\right\}_j, \qquad \frac{\partial g_y^2}{\partial j} = \{N\}\left\{g_y^2\right\}_j$$

The finite element formulation was implemented in a personal computer (Athlon 900 MHz, 512 Mb RAM) using the Matlab software. For a single modal analysis a typical CPU time is about 10 minutes. The geometric models, the attribution of physical properties and boundary conditions, the finite element unstructured mesh generation (using Delaunay algorithm) and graphic visualization of the electromagnetic fields were done using the LevSoft, which was developed in the Institute of Advanced Studies – IEAv/CTA for finite element applications [17].

IV. COUPLING EFFICIENCY CALCULATIONS

The coupling efficiency between a single-mode circular core optical fiber and a single-mode Ti:$LiNbO_3$ waveguide was calculated by the overlap integral of the spatial field distribution:

$$\Psi = \frac{\left|\iint E_f\, E_g\, dz\, dx\right|^2}{\iint \left|E_f\right|^2 dz\, dx \iint \left|E_g\right|^2 dz\, dx}, \quad (17)$$

where E_f and E_g are the electric fields in the fiber and in the optical waveguide, respectively.

For the circular core fiber, the field profile is well approximated by the Gaussian function [4]-[9]:

$$E_f(r) \propto \exp\left(-r^2/2\,a^2\right) \quad (18)$$

where $r^2 = x^2 + z^2$ and a is the mode radius of the fiber at the half-width-at-half-maximum field intensity.

Fig. 3 presents the fiber to waveguide coupling efficiency and the waveguide mode diameter in the transversal directions (W_x, W_z) as a function of the initial width of Ti-strip for different diffusion times. The following set of fixed parameters was assumed: H=80 nm, T=1050 °C, λ=1.523 μm and the fiber mode diameter $2a$=5 μm. For this particular case, the waveguide is single-mode for Ti-strip widths smaller than 7 μm for t=3 h and smaller than 10 μm for t=12 h. The coupling efficiency values reach approximately 92% on the single-mode region. However, for long diffusion times the maximum coupling efficiency condition is near the cutoff second mode.

The coupling efficiency and the mode diameters as a function of the initial Ti-strip thickness (H) and diffusion time are presented in Fig. 4 for W=5 μm, T=1050°C, λ=1.523 μm and $2a$=5 μm. When t=3 h, the waveguide is single-mode for $H \leq 95$ nm and the cutoff frequency for the fundamental mode is reached for $H \leq 55$ nm. For the case of $t \geq 6$ h, the propagation is only single-mode but the cutoff frequency changes to higher Ti thickness. In all cases the maximum coupling efficiency is approximately 92 %, however for $t = 6$ h the efficiency values presents low sensitivity to the thickness variations, allowing to simplify the Ti-strip deposition requirements.

Fig. 5 shows the coupling efficiency and the waveguide mode diameters as functions of both diffusion temperature and the diffusion time for W=5 μm, H=80 nm, λ=1.523 μm, and $2a$=5 μm. Again, the maximum coupling efficiency is about 92 % for each diffusion time considered. The maximum efficiency values are reached for temperatures between 1000°C and 1100°C and correspond to waveguide mode diameters near to 5 μm which is the mode diameter in the fiber.

Figs. 3-5 show the maximum values of coupling efficiency for different fabrication parameters. Even though, the related fiber positions are essential to define the geometrical parameters of the alignment grooves, which are manufactured either by chemical etching or laser ablation system. The Figs. 6(a)-6(c) present the center fiber position (z=0 μm, fixed) corresponding respectively to the data set of the Figs. 3-5. The simulations show that the fiber position changes around 1 μm with W or H variations. For temperature variations between 900°C and 1150°C the fiber position must be modified by ≈ 5 μm.

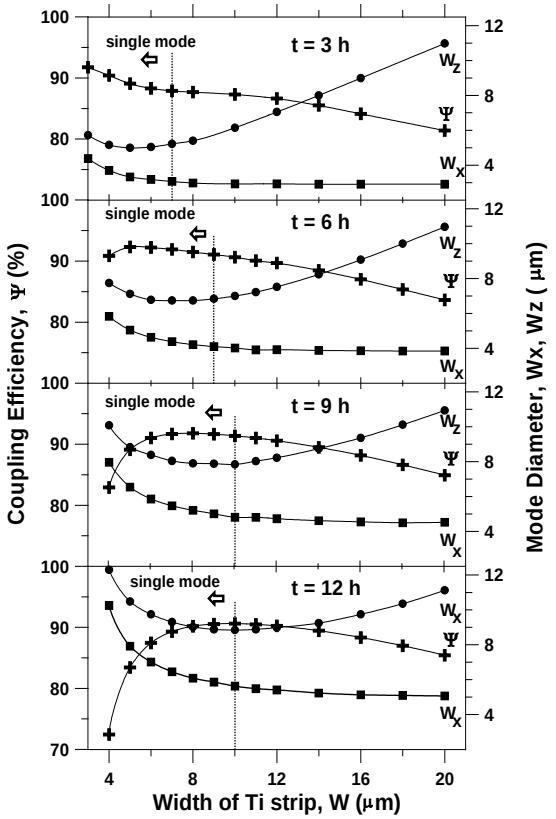

Fig. 3. The coupling efficiency and waveguide mode diameter as functions of the initial width of Ti-strip and the diffusion time.

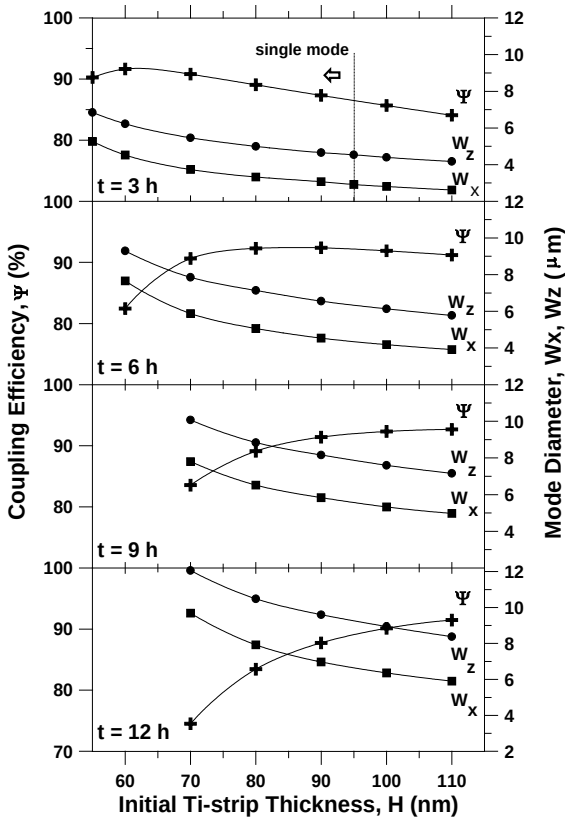

Fig. 4. The coupling efficiency and waveguide mode diameter as functions of the initial Ti-strip thickness and the diffusion time.

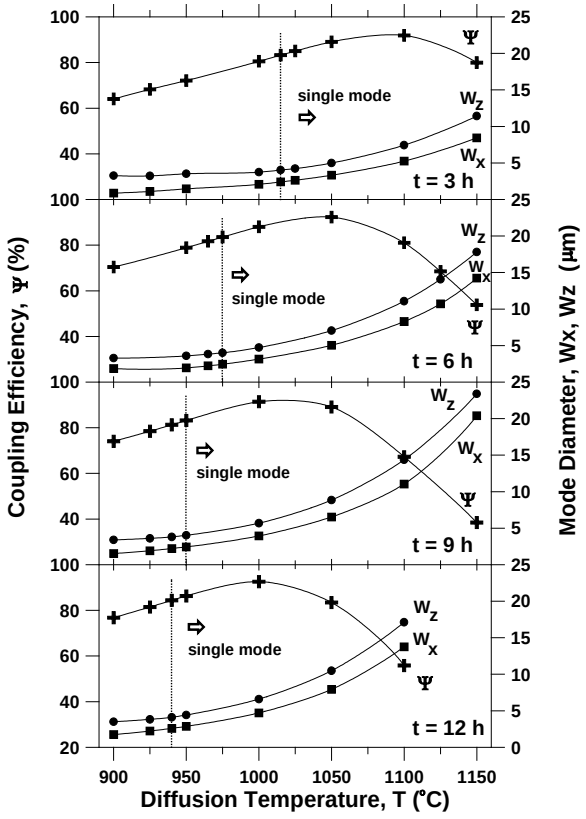

Fig. 5. The coupling efficiency and waveguide mode diameter as functions of the diffusion temperature and the diffusion time.

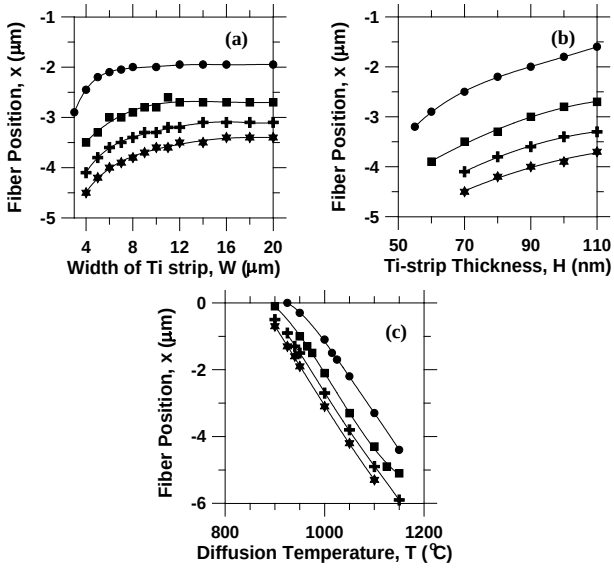

Fig. 6. The vertical center fiber position, x ($z = 0$ μm), corresponding to the maximum coupling efficiency as a function of the waveguide fabrication parameters. λ t = 3 h, ν t = 6 h, ✱ t = 9 h, and ✚ t = 12 h.

The alignment tolerances studies are illustrated in Fig. 7 in which the coupling efficiency is plotted against transversal offsets for the following fixed parameters: $2a$=5 μm, W=5 μm, H=80 nm, T=1050°C, and λ=1.523 μm. The mechanical tolerances were determined considering a maximum connection loss equal −1.0 dB (≈ 20.6 %).

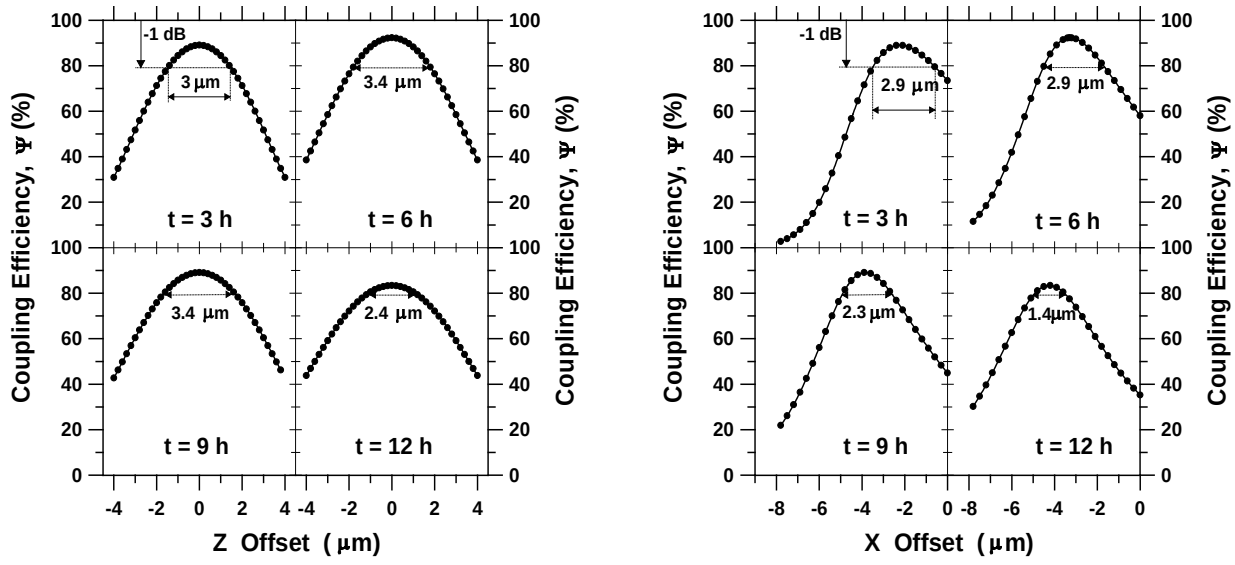

(a) (b)

Fig. 7. Coupling efficiency as a function of the transversal offset. (a) Offset in z-direction, (b) offset in x-direction.

TABLE II
COUPLING EFFICIENCY FOR COMMERCIAL OPTICAL FIBERS

λ (μm)	$2a$ (μm) fiber	n_{eff} guide	W_z (μm) guide	W_x (μm) guide	Ψ (%)
0.820	3.748	2.174061	4.28	2.758	88.517
1.060	5.092	2.159105	5.20	3.444	86.830
1.300	5.656	2.147652	6.14	4.215	89.234
1.550	6.718	2.138914	7.22	5.145	89.792

The results shown in the Figs. 3-7 were calculated for a typical fiber mode diameter ($2a$=5 μm) and the waveguide mode dimensions were calculated for λ=1.523 μm. By taking into account some commercial fiber characteristics is possible to obtain the attachment condition for special cases. Table II presents an example for four commercial fibers (manufactured by 3M, PM series) where the following fixed parameters were considered W=5 μm, H=80 nm, T=1050°C, and t=6 h.

I. CONCLUSIONS

The fiber-to-diffused waveguide coupling efficiency was calculated by using the finite element modal analysis for the Ti:$LiNbO_3$ waveguide. The effect of waveguide fabrication parameters on the coupling was verified. The relative fiber positions to obtain the maximum coupling efficiency were determined. This study permits the design of groove channels to attach and align the fiber-waveguide connection. The mechanical precision alignment requirements were determined by analyzing the fiber transversal offsets.

ACKNOWLEDGMENT

The authors wish to acknowledge the Fundação de Amparo à Pesquisa do Estado de São Paulo (FAPESP) by the partial support, process number 98/07789-7.

REFERENCES

[1] L. Eldada and J. T. Yardley, "Modal Analysis for Optimization of Single-Mode Waveguide Pigtailing and Fiber Splicing," *Appl. Opt.*, vol. 37, N. 33, pp.7747-7751, Nov. 1998.

[2] M. L. Tuma and G. Beheim, "Calculated Coupling Efficiency Between an Elliptical Fibres and a Silicon Oxynitride RIB Waveguide," *NASA Tech. Memo.* 106850, 1995.

[3] N. H. Zhu, X. S. Zheng, Y. K. Lin, and X. Yu, "Calculation of the field distribution of a Ti:$LiNbO_3$ Optical Waveguide and its Applications," *Optical and Quantum Electronics*, vol. 24, pp.737-743, 1992.

[4] S. Y. Wang and S. H. Lin, "High Speed III-V Electrooptic Waveguide Modulators at λ = 1.3 μm," *J. Lightwave Technol.*, vol. 6, N. 6, pp.758-771, Jun. 1988.

[5] E. J. Murphy, "Fiber Attachment for Guided Wave Devices," *Journal of Lightwave Technol.*, vol. 6, N. 6, pp.862-871, Jun. 1988.

[6] P. G. Suchoski Jr. and R. V. Ramaswamy, "Minimum-Mode-Size Low-Loss Ti:$LiNbO_3$ Channel Waveguides for Efficient Modulator Operation at 1.3 μm," *IEEE Journal of Quantum Electronics*, vol.23, N. 10, pp. 1673-1679, Oct. 1987.

[7] J. J. Veselka and S. K. Korotky, "Optimization of Ti:$LiNbO_3$ Optical Waveguides and Directional Coupler Switches for 1.56 μm Wavelength," *IEEE Journal of Quantum Electronics*, vol. 22, N. 6, pp.933-938, Jun. 1986.

[8] L. McCaughan and E. J. Murphy, "Influence of Temperature and Initial Titanium Dimensions of Fiber-Ti:$LiNbO_3$ Waveguide Insertion Loss at λ = 1.3 μm," *IEEE Journal of Quantum Electronics*, vol. 19, N. 2, pp.131-136, Feb. 1983.

[9] R. C. Alferness, V. R. Ramaswany, S. K. Korotky, M. D. Divino, and L.L. Buhl, "Efficient Single-Mode fiber to Titanium Diffused Lithium Niobate

Waveguide Coupling for $\lambda = 1.32\ \mu m$," *IEEE Journal of Quantum Electronics*, vol. 18, N. 10, pp. 1807-1813, Oct. 1982.

[10] M. Fukuma and J. Noda, "Optical Properties of Titanium-Diffused $LiNbO_3$ Strip Waveguides and Their Coupling-to-a Fiber Characteristics," *Applied Optics*, vol. 19, N. 4, pp.591-597, Feb. 1980.

[11] C. H. Bulmer, S. K. Sheem, R. P. Moeller, and W. K. Burns, "High-Efficient Flip-Chip Coupling Between Single-Mode Fibers and $LiNbO_3$ Channel Waveguides," *Applied Physics Letters*, vol.37, N. 4, pp.351-353, Aug. 1980.

[12] W. K. Burns and G. B. Hocker, "End Fire Coupling Between Optical Fibers and Diffused Channel Waveguides," *Applied Optics*, vol. 16, N. 8, pp. 2048-2050, Aug. 1977.

[13] M. A. R. Franco, A. Passaro, J. R. Cardoso, and J. M. Machado, "Finite Element Analysis of Anisotropic Optical Waveguide with Arbitrary Index profile," *IEEE Trans. on Magnetics*, vol. 35, pp. 1546-1549, May. 1999.

[14] D. Zhang, C. Chen, G. Ding, J. Zhang, and Y. Cui, "Dependence of Ti-Diffused Er:$LiNbO_3$ Laser Efficiency on Waveguide Fabrication Parameters and Pump Wavelength," *IEEE Journal of Quantum Electronics*, vol. 33, N. 7, pp.1231-1235, Jul. 1997.

[15] S. Fouchet, A. Carenco, C. Daguet, R. Guglielmi, and L. Riviere, "Wavelength Dispersion of Ti Induced Refractive Index Change in $LiNbO_3$ as a Function of Diffusion Parameters," *Journal of Lightwave Technol.*, vol. 5, N. 5, pp. 700-708, May. 1987.

[16] D. S. Smith, H. D. Riccius, and R. P. Edwin, "Refractive Indices of Lithium Niobate," *Opt. Commun.*, vol. 17, N. 3, pp. 332-335, Jun. 1976.

[17] N. M. Abe, A. Passaro, M. A. R. Franco, F. Sircilli, V. A. Serrão, D. H. Odan and F. J. R. Santos, "Um Sistema de Software para Análise de Dispositivos e Componentes de Óptica Integrada, Fibras Ópticas e Microondas," Proceedings of the V Congresso Brasileiro de Eletromagnetismo - CBMag 2002, Gramado – RS, November 04 a 06, Brazil, 2002.

Marcos Antonio Ruggieri Franco was graduated in Physics at Pontifícia Universidade Católica de São Paulo-Brazil (PUC-SP), in 1983. In 1991, he finished his Master Science degree in Nuclear Physics at Instituto de Física da Universidade de São Paulo-Brazil (IFUSP). In 1999, he received his doctorate in Electrical Engineering from the Escola Politécnica da Universidade de São Paulo-Brazil (POLI-USP). In 1987, he joined the research team of the Division of Applied Physics at Institute of Advanced Studies (IEAv) at Centro Técnico Aeroespacial (CTA). Since 2001, he is also associated professor of the pos-graduate course of Electronic and Computation Engineering from the Instituto Tecnológico de Aeronáutica (ITA). His major areas of interest are the application of the Finite Element Method for the design of electromagnetic devices such as microwave and optical waveguides, fiber optics, integrated optics, antennas and electromagnetic scattering problems.
(*email: marcos@ieav.cta.br*)

Laurentino Corrêa de Vasconcellos Neto, was graduated in Physical Science and Industrial Mechanical Engineering and pos-graduated in Optical Engineering. His Master Science was in Biomedical Engineering and his Doctorate was in Electrical Engineering obtained from the Escola Politécnica da Universidade de São Paulo-Brazil (POLI-USP). Since 1975, he is working at the Centro Técnico Aeroespacial as a researcher. Since 2001, he is associated professor of the pos-graduated course of Bioengineering at Universidade do Vale do Paraiba-UNIVAP, Brazil.
(*email: vasko@ieav.cta.br*)

José Márcio Machado obtained his Doctorate in Electrical Engineering from the Escola Politécnica da Universidade de São Paulo (1993). In 1985, he finished his Master Science at the Centro Brasileiro de Pesquisas Físicas (CBPF). Nowadays, he is professor of Mathematics at the Universidade do Estado de São Paulo–Brazil (UNESP-São José do Rio Preto) at Science Computation. His main researches interests are numerical methods, differential equations and applications for Physics, Mathematics and Engineering.
(*email: jmarcio@dcce.ibilce.unesp.br*)